Progress towards the FRIB-EDM^3-Frontend: A tool to provide radioactive molecules from isotope harvesting for fundamental symmetry studies

J. Ballof[a,b,*], N. Nusgart[a], P. Lalain[a], M. Au[b,c], R. Heinke[b], D. Leimbach[d], S. Stegemann[b], M. Schütt[b], S. Rothe[b], Jaideep T. Singh[a]

[a] *Facility for Rare Isotope Beams, Michigan State University, East Lansing, 48824, Michigan, USA*
[b] *CERN, Geneva 23, 1211, Switzerland*
[c] *Department of Chemistry, TRIGA-site, Johannes Gutenberg - University Mainz, Mainz, 55199, Germany*
[d] *University of Gothenburg, Gothenburg, 41296, Sweden*

Abstract

The under-construction FRIB-EDM^3-instrument was designed to study polar radioactive molecules (such as RaF) in transparent cryogenic solids by laser spectroscopy. The instrument is divided into a frontend- and a backend section. The frontend accepts an aqueous sample from isotope harvesting and provides a mass-separated molecular ion beam in an ultra-high vacuum environment. In the backend, the ions are guided into alkali-metal vapor and the resulting neutrals are co-deposited in a solid argon matrix to perform laser spectroscopy. This work addresses the frontend of the instrument. The efficient ionization of harvested radioisotopes from aqueous samples is achieved with a spray-ionization method. Subsequently, the molecular ion beam is analyzed by mass-to-charge ratio by a quadrupole mass filter. To verify the feasibility of the approach, numerical simulations with the COMSOL and SIMION packages have been conducted. While the former was applied to study transport in ion funnels, the latter was used to investigate ion beam transmission through the lower pressure sections. Following promising simulation results, a first experimental setup is under construction.

Keywords: Radioactive ion beams, Fundamental symmetries, Radioactive molecular beams, SIMION, COMSOL, RaF

1. Introduction

The study of radioactive molecules receives increasing attention due to their enhanced sensitivity to fundamental symmetry violations and Beyond Standard Model physics [1, 2]. In particular, ^{225}RaF has been proposed as powerful probe due to its enhanced Schiff-moment which facilitates experimental searches for a CP-violating permanent electric dipole moment. Recently, first preparatory experimental results on short-lived isotopes of the molecule were reported [3, 4, 5]. While the principle advantage of polar molecules over atomic probes is known for more than 30 years [6], the development of novel instruments is required to embark on such studies. At the Facility for Rare Isotope Beams (FRIB), the availability of suitable radioisotopes is being addressed by development of isotope harvesting techniques [7].

In this work, we introduce the frontend of the under-construction FRIB-EDM^3 instrument which will serve to ionize radiotracers from aqueous samples, enable their separation by mass-to-charge ratio, and subsequently guide them to the downstream experiment. The measurement precision of experiments pursuing searches for permanent electric dipole moments (see *e.g.*, ref. [8] for a review) is typically limited by statistical factors. A promising approach to maximize the number of simultaneously probed molecules is their introduction into a solid matrix. A measurement scheme was proposed aiming at the electron electric dipole moment of BaF embedded in solid rare-gas matrices [9] and first spectroscopic studies were conducted [10]. The FRIB-EDM^3 instrument aims at adapting the approach to investigations towards nuclear Schiff moments.

2. Instrument outline

The envisaged configuration of the FRIB-EDM^3-instrument is given in fig. 1 and was adapted from related instruments [11, 12, 13, 14, 15]. It consists of an electrospray ion source, ion optical elements to confine the ions in differentially pumped sectors, a quadrupole deflector, and a quadrupole mass filter. To avoid decomposition of the molecule in a downstream experiment, the instrument is designed such that ions are not accelerated beyond a kinetic ion energy of a few eV.

ElectroSpray Ion sources (ESI) are often used for the ionization of aqueous samples [16] and were found to be highly efficient in the nano-flow regime [17]. In an ESI, the aqueous sample is typically introduced with a syringe pump into a capillary which is positively biased to 2 kV to 5 kV. A spray of charged droplets emerges from the tip of the capillary. Electrodynamic ion funnels [18] are used to confine the droplets and allow for their desolvation. The first ion funnel is kept at a pressure of ca. 40 mbar. A second ion funnel enables further pressure reduction to ca. 1 mbar. Separation of isotopes by mass-to-charge ratio is achieved with a Quadrupole Mass Filter (QMF).

*Corresponding author
Email addresses: Jochen.Ballof@cern.ch (J. Ballof), nusgart@frib.msu.edu (N. Nusgart), singhj@frib.msu.edu (Jaideep T. Singh)

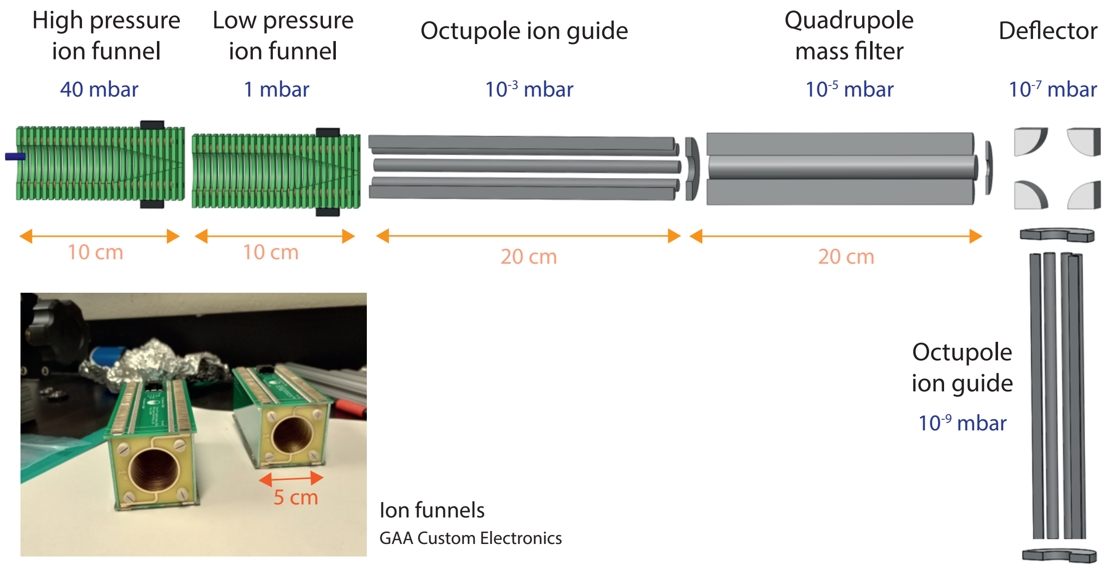

Figure 1: Schematic overview of the EDM^3-Frontend with inset photo of the ion funnels. The given dimensions are approximate.

Collisions of ions with the residual gas in the QMF should be avoided to enable efficient operation. Thus, a further reduction of pressure is required which is achieved via an additional differential pumping stage. Therein, the low-energy (few eV) ions are radially confined within an octupole ion guide which connects through an electrostatic lens to the quadrupole mass filter. The desired ions emerging from the ESI are accompanied by neutral species, *e.g.,* clusters of water molecules. Neutral species are vastly unaffected by the applied electric fields and propagate predominantly in a straight line through the setup. An electrostatic quadrupole deflector accounts for the suppression of the aforementioned contaminants. Consequently, the central axis of ion funnels and first octupole ion guide are offset. To achieve the final pressure required by the downstream experiment (10^{-9} mbar), an additional differential pumping section is added after the electrostatic deflector.

3. Ion funnel simulations

Electrodynamic ion funnels are often used for large biomolecules and are discriminating in mass-to-charge ratio of the ion. The high- and low-m/z cut-off properties depend on the ion funnel geometry and its operating conditions [19]. Within this work, we have conducted numerical simulations with the COMSOL Multiphysics 5.5 suite [20] to verify the applicability of commercially available ion funnels (GAA Custom Electronics) in the lower mass range. The species ^{225}RaF (244 g mol^{-1}) and its stable surrogate BaF (157 g mol^{-1}) are of particular interest.

A recent review about electrodynamic ion funnels is given in ref. [18]. A funnel consists of an array of ring electrodes and is divided into two sections. The inner diameter (ID) of the ring electrodes is constant in the entrance section to allow desolvation of droplets, and progressively narrows down towards the outlet. Ions are radially confined by radio-frequency (RF) signals which are applied with opposite polarity to neighboring electrodes. In addition, an electrostatic potential gradient (see table 1) is applied to guide ions from the inlet to the outlet. The last plate of a funnel (conductance limit) is supplied by a constant voltage only.

The available ion funnels (*cf.* fig. 1) are assembled out of 102 plates with a thickness of 0.5 mm, which are separated by a 0.5 mm gap. The inner diameter of the first 55 plates is constant and afterwards decreases towards the outlet from 25.4 mm to 2.5 mm.

The COMSOL simulation first solves for the electric potential distribution and applies these in a successive charged particle tracing study. Nitrogen at rest with ambient temperature and a pressure of 1.33 mbar was assumed as background gas, which is expected to closely resemble the environment of the low pressure ion funnel. The particle tracing simulation is initialized by creating ions in the inlet plane of a funnel with random velocity sampled from a Maxwellian distribution according to the assumed temperature of 20 °C. The ions propagate due to electrical forces while elastic ion-gas collisions are considered. The collision cross-sections of the alkaline earth mono fluorides were estimated with the projection-method of the Ion Mobility Spectrometry Suite (IMoS) [21] and fitted versus ion mass with an empirical function.

The parameters of the simulations are based on technical feasibility and are given in table 1. Resulting typical ion trajectories are shown in fig. 3 along with their kinetic energy. The conductance limiting plate was biased with −50 V relative to the last RF-driven plate to ease ion extraction from the funnel and avoid trapping of ions near the outlet.

The fate of an ion is either striking an electrode or traveling down the funnel axis and emerging from the outlet orifice. The obtained mass-dependent transmission, *i.e.*, ratio of transmitted vs. injected ions, is shown in fig. 2. Within the considered parameter range, transmission increases with increasing RF fre-

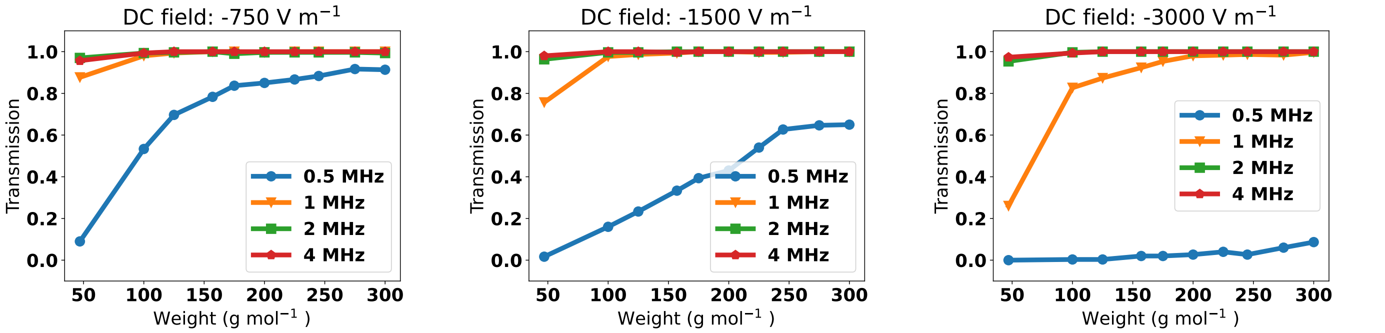

Figure 2: Simulated ion transmission through electrodynamic ion funnel obtained by COMSOL in dependence of ion mass, RF frequency and axial electrostatic (DC) field gradient. Nitrogen gas at rest having ambient temperature and a pressure of 1.33 mbar was assumed as background gas. Lines were added to guide the eye.

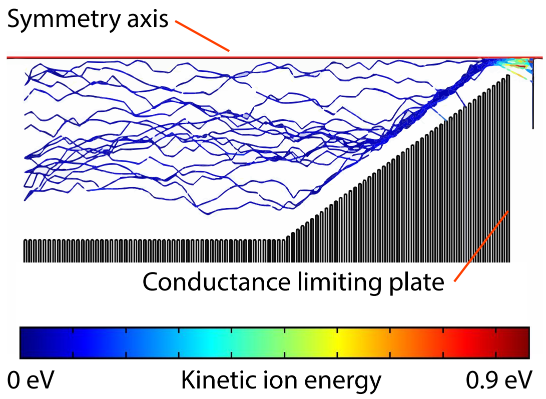

Figure 3: Typical ion trajectories in an electrodynamic ion funnel obtained by COMSOL. The color code represents the kinetic ion energy. The symmetry axis (rotational symmetry) is indicated. See text for details.

Table 1: Parameters of the ion funnel simulations

parameter	value	unit
ions per run	300	
RF voltage (peak-to-peak)	100	V
RF frequency	0.5 to 4	MHz
ion mass	100 to 300	g mol^{-1}
electrostatic potential gradient	7.5 to 30	V cm^{-1}
pressure	1.33	mbar

quency and ion mass. Barium mono fluoride (157 g mol^{-1}) as stable surrogate of radium mono fluoride is the lightest ion of interest. Unit transmission of BaF is predicted at an RF frequency of 1 MHz. The desired suppression of light contaminants can be adjusted by choice of the electrical potential gradient. At constant RF frequency, lowering the aforementioned gradient further suppresses the transmission of light masses.

4. Beam transport simulations

Ion transmission downstream the funnels (fig. 1) was investigated with the SIMION 8.2 ion optics modeling program [22, 23]. The geometry and driving voltages of model components were based on commercially available components offered by Process Insights (Extrel) and Beam Imaging Solutions. While the deflector geometry [24] was taken from the latter supplier, the remaining components were geared towards the Extrel portfolio. The radii of the quadrupole mass filter and octupole ion guide rods was assumed to be 9.5 mm and 1.1 mm, respectively. Electrostatic lenses were placed before and after ion guides and quadrupole mass filter with aperture diameters of 2.5 mm and 1.5 mm, respectively. The aforementioned lenses equally serve as conductance limit in the differentially pumped setup. Brubaker lenses are positioned adjacent to the entrance and exit of the quadrupole filter to reduce ion losses due to fringe fields [25]. Einzel lenses at entrance and exit of the deflector were used to focus the beam. Results of the simulation are given in fig. 4. The total transmission of the considered setup was estimated to be ca. 32% for the species of interest ($^{225}RaF^+$). A contamination of ca. 0.7% of the initial beam intensity on the higher mass $^{226}RaF^+$ is expected. The largest transmission loss can be attributed to the quadrupole mass filter. The latter equally impacts the downstream emittance due to the oscillating particle trajectories therein and causes losses in deflector and second ion guide. In these simulations, ion-gas interactions were neglected due to the relatively low pressure regime. Consideration of the aforementioned interactions might further affect ion transmission, in particular in the first octupole ion guide.

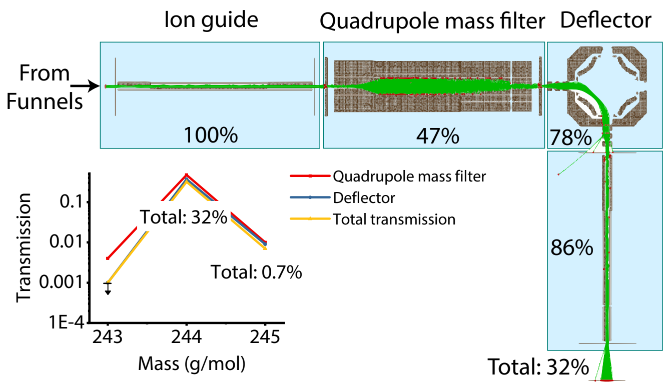

Figure 4: SIMION beamtransport simulation of the EDM^3 frontend. The ion transmission for each element is given. The inset shows transmission of the ion of interest ($^{255}RaF^+$) and contaminants of neighboring masses.

5. Conclusions and Outlook

Within this work, we have proposed an instrument for the ionization, mass separation and delivery of alkaline earth mono fluoride ions from aqueous solutions into an ultra-high vacuum environment. The ionization is achieved by an electrospray ion source in combination with electrodynamic ion funnels. The ions are confined in ion guides within a series of differential pumping stages. Detailed computational simulations were conducted which indicate the feasibility of the approach. Despite their typical application for large biomolecules, COMSOL simulations of the low pressure ion funnel indicate that commercially available ion funnels allow to access the desired mass range and efficient ion transfer is expected. Downstream the ion funnels, a transmission of ca. 32% is predicted through the remaining setup for ^{225}RaF by SIMION.

Following the promising simulation results, we have designed a prototype setup consisting of an electrospray ion source with heated inlet capillary, two consecutive ion funnels, an ion guide and a quadrupole mass filter, which is now under construction to further evaluate the design. In particular, gas-flow effects in the ion funnels and ion guides, ion source chemistry and space-charge limitations are among the study objectives.

Acknowledgments

The authors gratefully acknowledge support from Gordon Anderson (GAA Custom Electronics) regarding ion funnels and electronics. For fruitful discussions we would like to thank S. Schwarz, R. Ringle (both FRIB) and G. Koyanagi (York University, Canada). This work was supported by the U.S. DOE, Office of Science, Office of Nuclear Physics, under contract DE-SC0019015 and EU's Horizon 2020 Research and Innovation Programme under grant agreement number 861198 project 'LISA' (Laser Ionization and Spectroscopy of Actinides) Marie Sklodowska-Curie Innovative Training Network (ITN).

References

[1] N. R. Hutzler, A. Borschevsky, D. Budker, D. DeMille, V. V. Flambaum, G. Gabrielse, R. F. G. Ruiz, A. M. Jayich, L. A. Orozco, M. Ramsey-Musolf, M. Reece, M. S. Safronova, J. T. Singh, M. R. Tarbutt, T. Zelevinsky (2020). 10.48550/ARXIV.2010.08709.

[2] G. Arrowsmith-Kron, M. Athanasakis-Kaklamanakis, M. Au, J. Ballof, R. Berger, A. Borschevsky, A. A. Breier, F. Buchinger, D. Budker, L. Caldwell, C. Charles, N. Dattani, R. P. de Groote, D. DeMille, T. Dickel, J. Dobaczewski, C. E. Düllmann, E. Eliav, J. Engel, M. Fan, V. Flambaum, K. T. Flanagan, A. Gaiser, R. G. Ruiz, K. Gaul, T. F. Giesen, J. Ginges, A. Gottberg, G. Gwinner, R. Heinke, S. Hoekstra, J. D. Holt, N. R. Hutzler, A. Jayich, J. Karthein, K. G. Leach, K. Madison, S. Malbrunot-Ettenauer, T. Miyagi, I. D. Moore, S. Moroch, P. Navrátil, W. Nazarewicz, G. Neyens, E. Norrgard, N. Nusgart, L. F. Pašteka, A. N. Petrov, W. Plass, R. A. Ready, M. P. Reiter, M. Reponen, S. Rothe, M. Safronova, C. Scheidenberger, A. Shindler, J. T. Singh, L. V. Skripnikov, A. V. Titov, S.-M. Udrescu, S. G. Wilkins, X. Yang, Opportunities for fundamental physics research with radioactive molecules, 2023. URL: `https://arxiv.org/abs/2302.02165`. doi:10.48550/ARXIV.2302.02165.

[3] A. D. Kudashov, A. N. Petrov, L. V. Skripnikov, N. S. Mosyagin, T. A. Isaev, R. Berger, A. V. Titov, Ab initio study of radium monofluoride (RaF) as a candidate to search for parity- and time-and-parity–violation effects, Physical Review A 90 (2014) 052513. doi:10.1103/physreva.90.052513.

[4] S. Udrescu, A. Brinson, R. G. Ruiz, K. Gaul, R. Berger, J. Billowes, C. Binnersley, M. Bissell, A. Breier, K. Chrysalidis, T. Cocolios, B. Cooper, K. Flanagan, T. Giesen, R. de Groote, S. Franchoo, F. Gustafsson, T. Isaev, Á. Koszorús, G. Neyens, H. Perrett, C. Ricketts, S. Rothe, A. Vernon, K. Wendt, F. Wienholtz, S. Wilkins, X. Yang, Isotope shifts of radium monofluoride molecules, Physical Review Letters 127 (2021) 033001. doi:10.1103/physrevlett.127.033001.

[5] R. F. G. Ruiz, R. Berger, J. Billowes, C. L. Binnersley, M. L. Bissell, A. A. Breier, A. J. Brinson, K. Chrysalidis, T. E. Cocolios, B. S. Cooper, K. T. Flanagan, T. F. Giesen, R. P. de Groote, S. Franchoo, F. P. Gustafsson, T. A. Isaev, Á. Koszorús, G. Neyens, H. A. Perrett, C. M. Ricketts, S. Rothe, L. Schweikhard, A. R. Vernon, K. D. A. Wendt, F. Wienholtz, S. G. Wilkins, X. F. Yang, Spectroscopy of short-lived radioactive molecules, Nature 581 (2020) 396–400. doi:10.1038/s41586-020-2299-4.

[6] T. A. Isaev, R. Berger, Lasercooled radium monofluoride: A molecular all-in-one probe for new physics, 2013. URL: `https://arxiv.org/abs/1302.5682`. doi:10.48550/ARXIV.1302.5682, `https://arxiv.org/abs/1302.5682`.

[7] E. P. Abel, M. Avilov, V. Ayres, E. Birnbaum, G. Bollen, G. Bonito, T. Bredeweg, H. Clause, A. Couture, J. DeVore, M. Dietrich, P. Ellison, J. Engle, R. Ferrieri, J. Fitzsimmons, M. Friedman, D. Georgobiani, S. Graves, J. Greene, S. Lapi, C. S. Loveless, T. Mastren, C. Martinez-Gomez, S. McGuinness, W. Mittig, D. Morrissey, G. Peaslee, F. Pellemoine, J. D. Robertson, N. Scielzo, M. Scott, G. Severin, D. Shaughnessy, J. Shusterman, J. Singh, M. Stoyer, L. Sutherlin, A. Visser, J. Wilkinson, Isotope harvesting at frib: additionalopportunities for scientific discovery, J. Phys. G: Nucl. Part. Phys. 46 (2019) 100501. doi:10.1088/1361-6471/ab26cc.

[8] T. Chupp, M. Ramsey-Musolf, Electric dipole moments: A global analysis, Phys. Rev. C 91 (2015) 035502. URL: `https://link.aps.org/doi/10.1103/PhysRevC.91.035502`. doi:10.1103/PhysRevC.91.035502.

[9] A. C. Vutha, M. Horbatsch, E. A. Hessels, Orientation-dependent hyperfine structure of polar molecules in a rare-gas matrix: A scheme for measuring the electron electric dipole moment, Physical Review A 98 (2018) 032513. doi:10.1103/physreva.98.032513.

[10] S. J. Li, R. Anderson, A. C. Vutha, Baf molecules trapped in neon ice, 2022. doi:10.48550/ARXIV.2207.07279.

[11] S. Bag, R. G. Bhuin, R. R. J. Methikkalam, T. Pradeep, L. Kephart, J. Walker, K. Kuchta, D. Martin, J. Wei, Development of ultralow energy (1–10 eV) ion scattering spectrometry coupled with reflection absorption infrared spectroscopy and temperature programmed desorption for the investigation of molecular solids, Review of Scientific Instruments 85 (2014) 014103. doi:10.1063/1.4848895.

[12] O. Hadjar, P. Wang, J. H. Futrell, Y. Dessiaterik, Z. Zhu, J. P. Cowin, M. J. Iedema, J. Laskin, Design and performance of an instrument for soft landing of biomolecular ions on surfaces, Analytical Chemistry 79 (2007) 6566–6574. doi:10.1021/ac070600h.

[13] N. de Ruette, M. Wolf, L. Giacomozzi, J. D. Alexander, M. Gatchell, M. H. Stockett, N. Haag, H. Zettergren, H. T. Schmidt, H. Cederquist, DESIREE electrospray ion source test bench and setup for collision induced dissociation experiments, Review of Scientific Instruments 89 (2018) 075102. doi:10.1063/1.5030528.

[14] J. J. Melko, S. G. Ard, N. S. Shuman, R. E. Pedder, C. R. Taormina, A. A. Viggiano, Coupling an electrospray source and a solids probe/chemical ionization source to a selected ion flow tube apparatus, Review of Scientific Instruments 86 (2015) 084101. doi:10.1063/1.4927716.

[15] C. Hamann, R. Woltmann, I.-P. Hong, N. Hauptmann, S. Karan, R. Berndt, Ultrahigh vacuum deposition of organic molecules by electrospray ionization, Rev. Sci. Instrum. 82 (2011) 033903.

[16] J. B. Fenn, M. Mann, C. K. Meng, S. F. Wong, C. M. Whitehouse, Electrospray ionization-principles and practice, Mass Spectrometry Reviews 9 (1990) 37–70. doi:10.1002/mas.1280090103.

[17] I. Marginean, J. S. Page, A. V. Tolmachev, K. Tang, R. D. Smith, Achieving 50% ionization efficiency in subambient pressure ionization with nanoelectrospray, Analytical Chemistry 82 (2010) 9344–9349.

doi:10.1021/ac1019123.
[18] R. T. Kelly, A. V. Tolmachev, J. S. Page, K. Tang, R. D. Smith, The ion funnel: Theory, implementations, and applications, Mass Spectrometry Reviews 29 (2010) 294–312. doi:10.1002/mas.20232.
[19] S. A. Shaffer, D. C. Prior, G. A. Anderson, H. R. Udseth, R. D. Smith, An ion funnel interface for improved ion focusing and sensitivity using electrospray ionization mass spectrometry, Analytical Chemistry 70 (1998) 4111–4119. doi:10.1021/ac9802170.
[20] Comsol multiphysics, 2023. URL: `https://www.comsol.com/`, (online accessed 16/01/2023).
[21] Ion mobility spectrometry suite, 2023. URL: `https://www.imospedia.com/imos/`, (online accessed 16/01/2023).
[22] D. A. Dahl, simion for the personal computer in reflection, International Journal of Mass Spectrometry 200 (2000) 3–25. doi:10.1016/s1387-3806(00)00305-5.
[23] Comsol multiphysics, 2023. URL: `https://simion.com/`, (online accessed 16/01/2023).
[24] H. D. Zeman, Deflection of an ion beam in the two-dimensional electrostatic quadrupole field, Review of Scientific Instruments 48 (1977) 1079–1085. doi:10.1063/1.1135188.
[25] W. M. Brubaker, Auxiliary electrodes for quadrupole mass filters, 1964. United States Patent, US3129327A.